

On the feedback structure of wideband piezoelectric shunt damping systems

S O Reza Moheimani, Andrew J Fleming and Sam Behrens

School of Electrical Engineering and Computer Science, University of Newcastle,
NSW, Australia

E-mail: reza@ee.newcastle.edu.au

Received 22 October 2001, in final form 17 October 2002

Published 10 January 2003

Online at stacks.iop.org/SMS/12/49

Abstract

This paper studies the feedback structure associated with piezoelectric shunt damping systems and introduces a new impedance structure for multi-mode piezoelectric shunt damping. The impedance is shown to be realizable using passive circuit components and digital implementation of the associated admittance transfer function is discussed.

(Some figures in this article are in colour only in the electronic version)

1. Introduction

Piezoelectric transducers are under investigation as actuators and sensors for vibration control in flexible structures. Piezoelectric materials in current use include poly-vinylidene fluoride (PVDF), a semi-crystalline polymer film and lead zirconate titanate (PZT), a piezoelectric ceramic material. These materials strain when exposed to a voltage and conversely produce a voltage when strained. The piezoelectric property is due to the permanent dipole nature of the materials, which is induced by exposing the material to a strong electric field while the material is being manufactured. For a detailed discussion of the electromechanical properties of these materials, the reader is referred to [1–3].

For vibration control purposes, piezoelectric transducers are bonded to the body of the base structure using strong adhesive material. These piezoelectric transducers can be used as sensors, actuators or both. In a typical active control problem, a piezoelectric transducer is used as an actuator. A sensor is used to measure vibration of the base structure and then a control voltage is applied to the piezoelectric actuator to minimize the unwanted vibration of the base structure.

An alternative approach is passive control, which is also referred to as piezoelectric shunt damping. The piezoelectric transducer is shunted by a passive electric circuit that acts as a medium for dissipating the mechanical energy of the base structure. In their original work Hagood and von Flotow [4, 5] suggested that a series R – L circuit attached across the conducting surfaces of a piezoelectric transducer can be tuned to dissipate mechanical energy of the base structure. They demonstrated the effectiveness of this technique by

tuning the resulting R – L – C circuit to a specific resonance frequency of the base structure. Furthermore, they proposed a method to determine an effective value for the resistive element.

In [6] it was demonstrated that a parallel R – L circuit could be shunted to the piezoelectric transducer for vibration reduction purposes and it was shown that similar results to the series case could be obtained. Later, the same author demonstrated that the concept could be extended to allow for multiple-mode shunt damping by introducing current blocking circuits inside each R – L branch [7, 8]. The problem with this technique, however, is that the size of the shunting circuit increases rapidly as the number of modes that are to be shunt dampened is increased. Reference [9] suggests a more practical shunt circuit for multiple mode piezoelectric shunt damping by using current-flowing circuits in each branch. An alternative multi-mode shunt damping circuit was suggested by Hollkamp [10]. Although the author conjectures the effectiveness of this circuit, no straightforward method for determining the circuit components is proposed.

One of the major difficulties that often arises in implementing these shunt impedances is the fact that one may need to have access to rather large inductors if the low-frequency modes are to be shunt dampened. The mainstream approach to addressing this problem appears to be centered around electronic implementation of these inductors using Gyrator circuits [11]. This may be a reasonable proposition if a very small number of modes are to be shunt dampened. However, for a large number of modes a more practical solution is needed.

The synthetic impedance circuit suggested in [12] is an effective means of digital implementation of an impedance

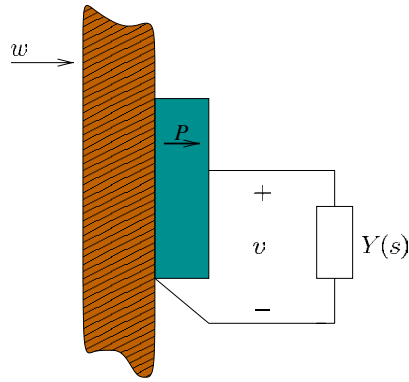


Figure 1. A piezoelectric laminate shunted to an admittance $Y(s)$.

circuit for piezoelectric shunt damping. This circuit allows us to implement any admittance transfer function, as long as the transfer function is stable, and at least proper. Indeed the circuit may be used to implement active shunts, as opposed to purely passive shunts. For an overview of current active/passive techniques, the reader is referred to [13].

Compared to other piezoelectric shunt damping techniques which are based on intuitive ideas, this paper presents a systematic way of designing the shunt impedance, as well as a thorough analysis of the feedback structure associated with the piezoelectric shunt damping systems.

The remainder of the paper continues as follows. Section 2 clarifies the feedback nature of the piezoelectric shunt damping systems. Section 3 introduces a new impedance structure for the purpose of piezoelectric shunt damping. It is explained why this specific structure may prove efficient in suppressing vibrations of structures. Section 4 contains a proof of closed-loop stability under the proposed impedance. Section 5 discusses some properties of the proposed admittance structure while section 6 discusses the robustness issues. Section 7 is concerned with the problem of optimal tuning of the shunting admittance. Section 8 includes our experimental results, and section 9 concludes the paper.

2. Feedback problem associated with a shunted piezoelectric laminate structure

Let us consider the system depicted in figure 1. Here a piezoelectric transducer is attached to the surface of a flexible structure using strong adhesive material. The piezoelectric transducer is shunted to an electrical admittance, $Y(s)$. The vector P signifies the direction of polarization vector of the piezoelectric material. As the structure deforms, possibly due to a disturbance $w(s)$, an electric charge distribution appears inside the piezoelectric crystal. This manifests itself in the form of a voltage difference across the conducting surfaces of the piezoelectric transducer, $v(s)$, which in turn causes the flow of electric current, $i(s)$, through the admittance. This causes a loss of energy. Hence, the electric admittance may be thought of as a means of extracting mechanical energy from the base structure via the piezoelectric transducer.

To make the discussion clearer, let us look at the system in more detail. Figure 2 depicts the electrical equivalent of the piezoelectric transducer [14]. If the admittance is removed

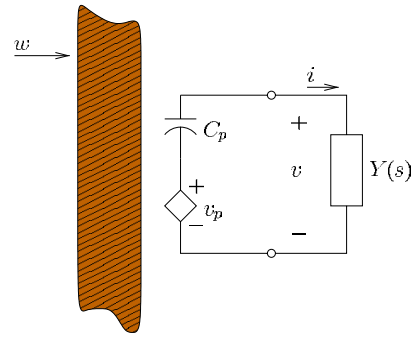


Figure 2. Electrical equivalent of the system in figure 1.

from the circuit, i.e. if the piezoelectric transducer is left open circuited, then the voltage measured across the conducting terminals of the piezoelectric transducer is equivalent to $v_p(s)$. This voltage is entirely due to the disturbances acting on the structure and/or non-zero initial conditions. It should be clear that as long as the base structure is not at rest, $v_p(s)$ may be non-zero. To this end, let us assume that $v_p(s)$ is related to $w(s)$ via a transfer function $G_{vw}(s)$. That is,

$$v_p(s) = G_{vw}(s)w(s), \quad Y(s) = 0. \quad (1)$$

The condition $Y(s) = 0$ in (1) emphasizes that this equation is valid only if the two terminals of the piezoelectric transducer are left open circuited.

Now, let us assume that there are no disturbances acting on the structure. Rather, allow us to assume that a voltage source is attached across the conducting terminals of the piezoelectric transducer. In this case, the voltage $v_p(s)$ is entirely due to $v(s)$ and is related to $v(s)$ via a transfer function $G_{vv}(s)$. That is,

$$v_p(s) = G_{vv}(s)v(s), \quad w(s) = 0. \quad (2)$$

The transfer function $G_{vv}(s)$ may be written in the general form

$$G_{vv}(s) = - \sum_{i=1}^{\infty} \frac{\gamma_i}{s^2 + 2\zeta_i\omega_i s + \omega_i^2} \quad (3)$$

where

$$\gamma_i > 0 \quad \text{for } i = 1, 2, \dots$$

To this end, it should be pointed out that the specific form of $G_{vv}(s)$ above is due to the collocated nature of the transfer function. In other words, if an identical piezoelectric patch is collocated with the shunted piezoelectric transducer, the voltage induced in the second transducer will be equivalent, but 180° out of phase with $v_p(s)$: for example, see [15, 16]. Also, note that if the piezoelectric transducer is attached to the structure such that vector P is pointing in the opposite direction, the negative sign in (3) should be removed. If the base structure is disturbed by $w(s)$ and a voltage $v(s)$ is simultaneously applied across the terminals of the piezoelectric transducer then due to the linearity of the system we may write

$$v_p(s) = G_{vw}(s)w(s) + G_{vv}(s)v(s). \quad (4)$$

From equation (4) it can be deduced that while the disturbance $w(s)$ is disturbing the base structure, the voltage

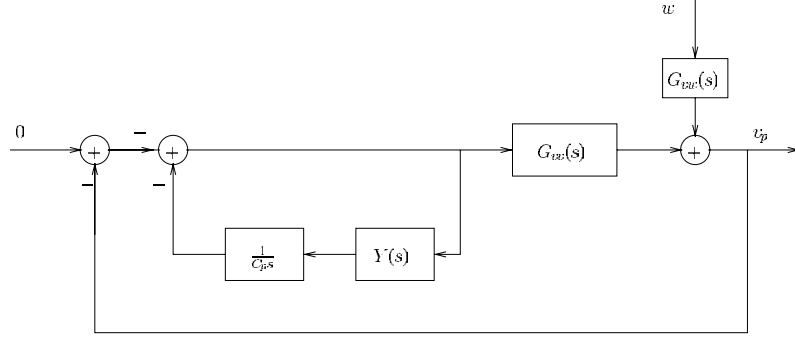


Figure 3. The feedback structure associated with the shunt damping problem in figure 2.

$v(s)$ applied across the piezoelectric terminals may be used to reduce the effect of this unwanted disturbance. In a typical feedback control problem, a sensor is used to measure a property of the structure for feedback. This may be the acceleration at some point, as measured by an accelerometer, or even the voltage measured at the open terminals of another piezoelectric transducer attached to the structure at a different point.

Shunting the piezoelectric transducer with the admittance $Y(s)$, as in figure 2, removes the need for an additional sensor. This, however, is achieved at the expense of having to deal with a more complicated feedback control problem.

To visualize the underlying feedback control structure, we need to identify a number of variables such as the control signal, the measurement, the disturbance and the physical variable that is to be regulated.

The underlying feedback structure can be identified by noticing that the current may be written as

$$i(s) = (v_p(s) - v(s))C_p s. \quad (5)$$

Furthermore,

$$i(s) = Y(s)v(s). \quad (6)$$

Equations (4)–(6) suggest the feedback structure depicted in figure 3. The figure suggests a rather complicated feedback structure as the controller, $Y(s)$, is itself inside an inner feedback loop.

Now, consider a system consisting of a base structure along with two piezoelectric transducers attached to either sides of the base structure in a collocated manner as in figure 4. Such a system is easily realizable in a laboratory. Indeed, our experimental results in section 8 are performed on a similar system. If the two piezoelectric transducers are identical, we may write

$$G_{vw}(s) = -G_{vv}(s).$$

Therefore, the block diagram in figure 3 may be reduced to that shown in figure 5.

3. A new impedance structure for piezoelectric shunt damping

Over the past ten years, a number of impedance structures have been suggested in the literature. This includes the single-mode shunt damping impedance proposed in [4–6] and several modifications of this technique to allow for multi-mode

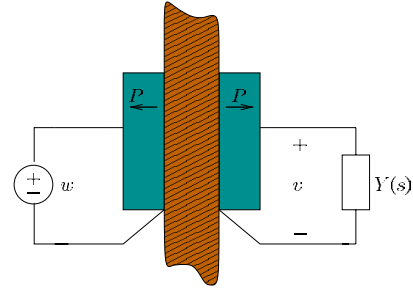


Figure 4. A structure with collocated piezoelectric transducers.

shunt damping [7, 8, 10]. This paper proposes a new class of admittances suitable for multi-mode piezoelectric shunt damping. Furthermore, stability and robustness properties of this class of admittances are analyzed and studied.

In the previous section we demonstrated that the piezoelectric shunt damping problem is equivalent to a feedback control problem with a very specific feedback structure. This understanding of the underlying feedback structure allows us to interpret the existing results in the literature in a meaningful way. Furthermore, it enables us to make new contributions to the field in the form of generating new classes of high-performance shunt damping impedance structures.

Notice that in figure 3 the closed-loop transfer function from the disturbance input $w(s)$ to $v_p(s)$ can be written as

$$T_{v_p w}(s) = \frac{v_p(s)}{w(s)} = \frac{G_{vw}(s)}{1 + K(s)\tilde{G}_{vv}(s)} \quad (7)$$

where

$$\tilde{G}_{vv}(s) = -G_{vv}(s)$$

and

$$K(s) = \frac{1}{1 + \frac{Y(s)}{C_p s}}. \quad (8)$$

Given the common-pole property of the transfer functions associated with the base structure, regardless of the nature of the disturbance, $G_{vw}(s)$ must have poles that are identical to those of $\tilde{G}_{vv}(s)$. Therefore, the role of the shunting admittance $Y(s)$ is to move the closed-loop poles of the system deeper into the left half-plane, i.e. to add more damping to each mode.

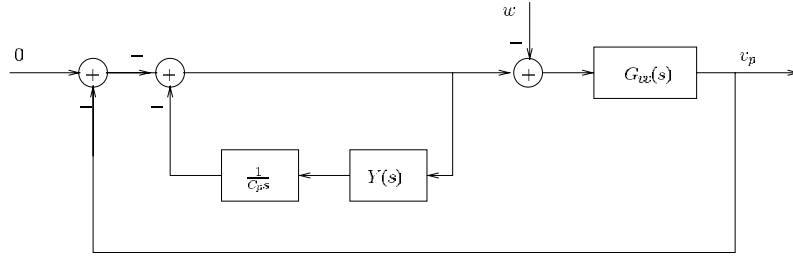


Figure 5. The feedback structure with the disturbance applied to the collocated piezoelectric transducer.

An effective admittance structure for this purpose is

$$Y(s) = \frac{\sum_{i=1}^N \frac{\alpha_i \omega_i^2}{s^2 + 2d_i \omega_i s + \omega_i^2}}{1 - \sum_{i=1}^N \frac{\alpha_i \omega_i^2}{s^2 + 2d_i \omega_i s + \omega_i^2}} C_p s \quad (9)$$

where

$$\alpha_i \geq 0, \quad d_i > 0, \quad i = 1, 2, \dots, N$$

and

$$\sum_{i=1}^N \alpha_i = 1. \quad (10)$$

An immediate choice for the α is $\alpha_i = \frac{1}{N}$ for $i = 1, 2, \dots, N$. This will ensure that condition (10) is satisfied. It is straightforward to verify that for the admittance structure defined in (9), the effective controller expression in (8) will be

$$K(s) = 1 - \sum_{i=1}^N \frac{\alpha_i \omega_i^2}{s^2 + 2d_i \omega_i s + \omega_i^2}. \quad (11)$$

This, in turn can be shown to be equivalent to

$$K(s) = \sum_{i=1}^N \frac{\alpha_i s(s + 2d_i \omega_i)}{s^2 + 2d_i \omega_i s + \omega_i^2}. \quad (12)$$

It should be possible to imagine why this specific structure may be quite effective in reducing unwanted vibrations of the base structure. Flexible structures are inherently highly resonant systems whose dynamics consist of a large number of very lightly damped modes. The admittance suggested in (9), once shunted to the piezoelectric transducer with the piezoelectric capacitance of C_p , will result in an equivalent feedback control problem where the controller $K(s)$ is defined as in (12). It can be observed that this controller has a highly resonant structure dictated by the damping factors d_1, \dots, d_N . The controller applies a high gain at each specific resonant frequency. This is done by applying a very narrow bandpass filter around each resonant frequency of the base structure.

To see the connections with the earlier work, we point out that if $N = 1$, then the controller may be tuned only to one specific resonant frequency, say ω_ℓ . In this case, it can be shown that

$$Y(s) = \frac{\omega_\ell^2 C_p}{s + 2d_\ell \omega_\ell}.$$

Hence, $Y(s)$ effectively represents the series connection of a resistor $R = \frac{2d_\ell}{\omega_\ell C_p}$ with an inductor $L = \frac{1}{\omega_\ell^2 C_p}$ shunted across the piezoelectric transducer terminals. This

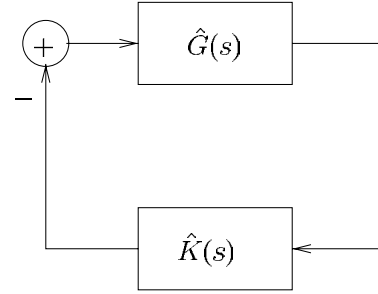


Figure 6. Equivalent system for study of closed-loop stability.

is the original single-mode shunt damping circuit proposed by Hagood and von Flotow [4]. Based on this observation, one may argue that $Y(s)$ in (9) effectively generates a phase and gain relationship around each resonant frequency that is similar to those generated by a R - L circuit tuned to that specific resonant frequency.

4. Closed-loop stability

In this section we study stability properties of the proposed shunting impedance. By inspection, it can be verified that the closed-loop stability of the system in figure 3 is equivalent to the stability of the system in figure 6 with

$$\hat{G}(s) = -s G_{vv}(s) = \sum_{i=1}^M \frac{\gamma_i s}{s^2 + 2\zeta_i \omega_i s + \omega_i^2} \quad (13)$$

and

$$\hat{K}(s) = \sum_{i=1}^N \frac{\alpha_i (s + 2d_i \omega_i)}{s^2 + 2d_i \omega_i s + \omega_i^2}.$$

The proof of closed-loop stability is rather straightforward and is based on the observation that $\hat{K}(s)$ is a strictly positive real (SPR) transfer function, i.e. $\hat{K}(j\omega) + \hat{K}(-j\omega) > 0$ for all $\omega \in \mathbf{R}$ and $\hat{G}(s)$ is a positive real (PR) transfer function, i.e. $\hat{G}(j\omega) + \hat{G}(-j\omega) \geq 0$ for all $\omega \in \mathbf{R}$. The feedback connection of two SISO systems where one is a SPR and the other is a PR transfer function is stable with a guaranteed gain margin of infinity (see chapter 10 of [17]). Therefore, the admittance suggested in (9) results in a closed-loop system that is stable with favorable stability margins.

It should be pointed out that (13) with M arbitrarily large, i.e. $M \gg N$, is a reasonable finite-dimensional approximation of (3) (see [18]).

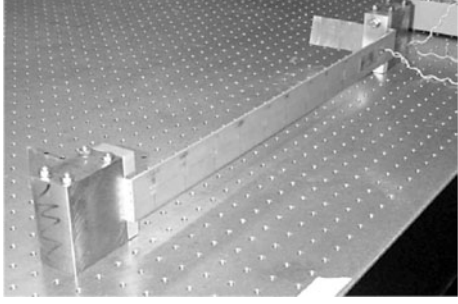


Figure 7. Piezoelectric laminated simply supported beam.



Figure 8. Piezoelectric laminated plate bounded structure.

5. Properties of the proposed admittance and implementation issues

Our ultimate goal is to implement the admittance $Y(s)$ digitally using the synthetic admittance circuit proposed in [12]. For this to be achievable in an efficient way, $Y(s)$ must satisfy a number of conditions. It should be a stable transfer function and it should be at least proper, and preferably strictly proper with a bandwidth that is not excessively larger than that of the highest in-bandwidth mode of the base structure that is to be controlled. In this section we study the structure of the proposed admittance and will show that it satisfies all the above conditions.

We first study the stability of $Y(s)$. This can be verified by observing that the Nyquist plot of

$$-\sum_{i=1}^M \frac{\alpha_i \omega_i^2}{s^2 + 2d_i \omega_i s + \omega_i^2} \quad (14)$$

with $M \gg N$ will never cross the critical point, $-1 + j0$. This, along with the feedback structure of $Y(s)$ in (9), establishes the stability of the admittance $Y(s)$.

Next, we note that the admittance $Y(s)$ can be written as

$$Y(s) = \frac{\sum_{i=1}^N \frac{C_p \alpha_i \omega_i^2 s}{s^2 + 2d_i \omega_i s + \omega_i^2}}{\sum_{i=1}^N \frac{\alpha_i s(s + 2d_i \omega_i)}{s^2 + 2d_i \omega_i s + \omega_i^2}} = \frac{H(s)}{J(s)}.$$

Now it can be verified that the numerator transfer function, $H(s)$, is a positive real transfer function, which means

$$-\frac{\pi}{2} \leq \angle H(s) \leq \frac{\pi}{2}.$$

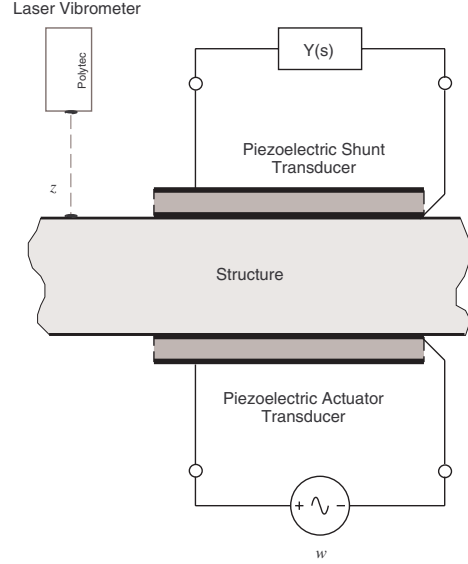


Figure 9. The experimental structure with collocated piezoelectric transducers.

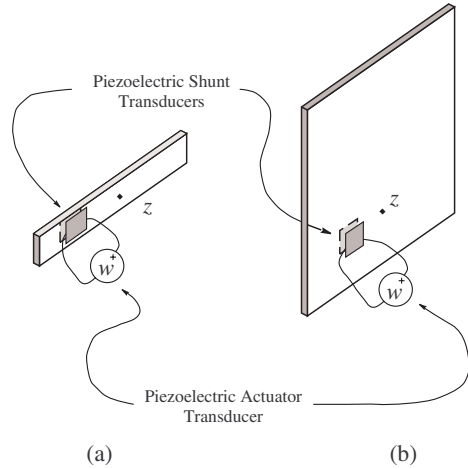


Figure 10. Experimental piezoelectric laminated structures: (a) beam and (b) plate. Note that w is the applied disturbance actuator voltage and z is the displacement at some point on the structure.

Furthermore, it can be verified that

$$0 < \angle J(s) < \pi.$$

Hence, we may conclude that

$$-\frac{\pi}{2} < \angle Y(s) < \frac{\pi}{2},$$

which means that $Y(s)$ is a SPR transfer function, i.e. the Nyquist plot of $Y(s)$ is confined to the right half of the complex plane. An implication of this observation is that $Y(s)$ is indeed realizable using purely passive circuit components, i.e. resistors, inductors and capacitors. Such a circuit may be realized by observing that $Y(s)$ can be written as

$$Y(s) = \frac{C_p \sum_{i=1}^N \alpha_i \omega_i^2 \prod_{\ell=1, \ell \neq i}^N (s^2 + 2d_\ell \omega_\ell s + \omega_\ell^2)}{\sum_{i=1}^N \alpha_i (s + 2d_i \omega_i) \prod_{\ell=1, \ell \neq i}^N (s^2 + 2d_\ell \omega_\ell s + \omega_\ell^2)}. \quad (15)$$

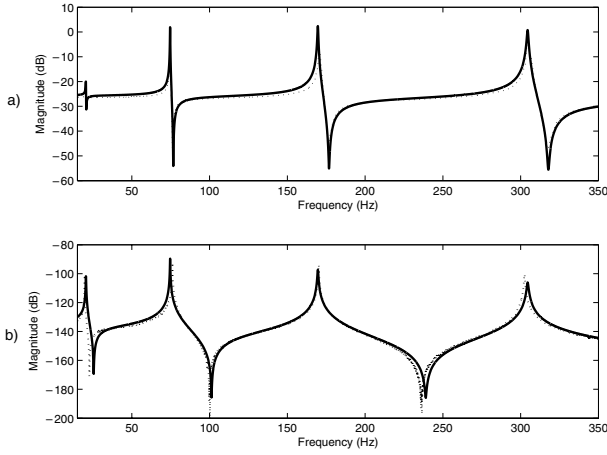


Figure 11. Frequency response (a) $|G_{vv}(s)|$ and (b) $|G_{zw}(s)|$, for the piezoelectric laminated beam structure. Experimental data (\cdots) and model obtained using subspace-based system identification (—).

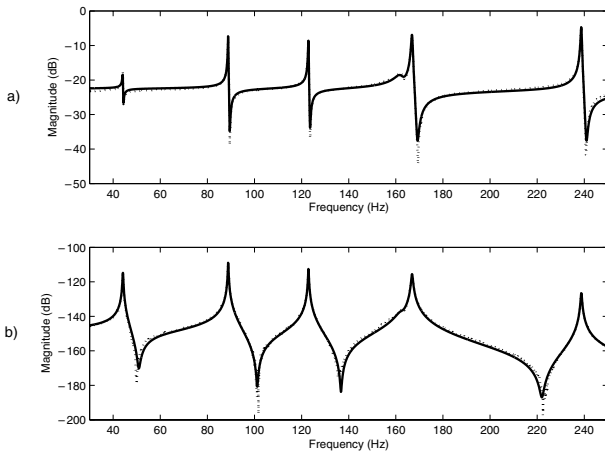


Figure 12. Frequency response (a) $|G_{vv}(s)|$ and (b) $|G_{zw}(s)|$, for the piezoelectric laminated plate structure. Experimental data (\cdots) and model obtained using subspace-based system identification (—).

Table 1. Summary of experimental amplitude reduction for both beam and plate structures.

| Mode | Beam (dB) | Plate (dB) |
|------|-----------|------------|
| 1 | 2.0 | 2.5 |
| 2 | 16.2 | 13.5 |
| 3 | 19.9 | 11.0 |
| 4 | 24.1 | — |
| 5 | — | 12.9 |
| 6 | — | 14.8 |

6. Robustness issues

An interesting property of the admittance proposed in (9) is its good robustness properties. To make this clearer we point out that under (9) the closed-loop system is stable with a gain margin of infinity. Therefore, the spill-over effect due to the existence of out-of-bandwidth modes will not destabilize the closed-loop system. As a matter of fact, the spill-over effect will be minimal since the admittance, and hence the resulting

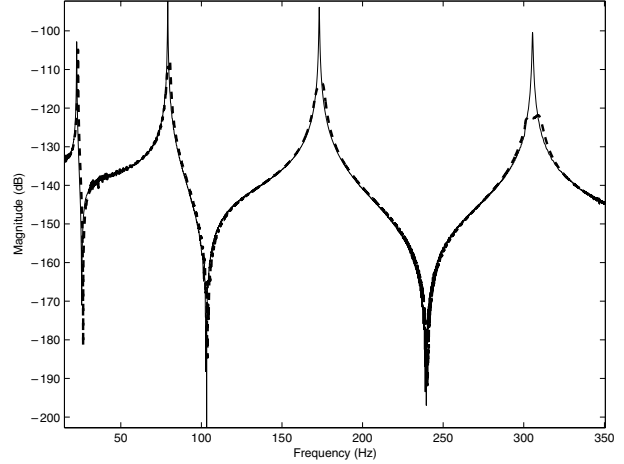


Figure 13. Experimental beam undamped (—) and damped (---) magnitude response of $G_{zw}(s)$.

equivalent controller $K(s)$ in (8), has a highly resonant nature.

The structure of the admittance $Y(s)$ is such that if the resonant frequencies $\omega_1, \dots, \omega_N$ are slightly different from the actual resonant frequencies of the base structure, closed-loop stability is guaranteed. This is a favorable property as these resonant frequencies are known to change with temperature, changing load, etc.

A particularly important robustness feature of the proposed admittance structure is that it maintains closed-loop stability even if the value of the piezoelectric capacitance in (9) is estimated incorrectly. A proof of this claim follows.

Let us assume that the actual value of the piezoelectric capacitance is C_p , while our estimate of it is $\hat{C}_p = \eta C_p$. Therefore, the admittance expression in (9) should be modified to

$$Y(s) = \frac{\sum_{i=1}^N \frac{\alpha_i \omega_i^2}{s^2 + 2d_i \omega_i s + \omega_i^2}}{1 - \sum_{i=1}^N \frac{\alpha_i \omega_i^2}{s^2 + 2d_i \omega_i s + \omega_i^2}} \hat{C}_p s.$$

Arguing along similar lines to section 4, we may say that the stability of the resulting closed-loop system is equivalent to the stability of the system in figure 6 with

$$\hat{G}(s) = -sG_{vv}(s)$$

and

$$\hat{K}(s) = \frac{1}{1 + \frac{\eta}{s} \tilde{Y}(s)}$$

with

$$\tilde{Y}(s) = \frac{1}{C_p} Y(s).$$

We have already established that $Y(s)$ is a SPR transfer function. Therefore strict positive realness of $\tilde{Y}(s)$ follows immediately. Now, it can be proved that $\hat{K}(s)$ is stable and that $\hat{K}(j\omega) + \hat{K}(-j\omega) > 0$ for all $\omega \in \mathbf{R}$. Therefore, $\hat{K}(s)$ is itself a SPR system. Given that $\hat{G}(s)$ is a PR system, we may conclude that the closed-loop system is stable for any $\eta > 0$.

To this end we point out that although the closed-loop system will not be destabilized, the performance of the system may severely deteriorate as η deviates from one.

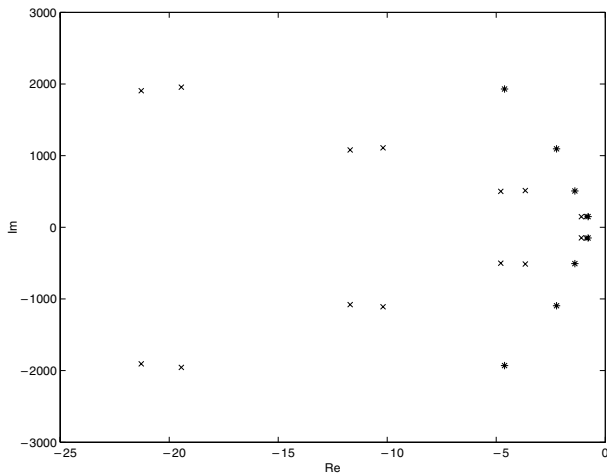


Figure 14. Simulated open-loop (*) and closed-loop (x) poles of the piezoelectric laminated beam.

7. Optimal tuning of the admittance

The structure of the admittance in (9) guarantees closed-loop stability of the system. In order to achieve good performance, appropriate values for the damping parameters d_1, d_2, \dots, d_N need to be determined. This may be done by seeking a solution to the following optimization problem:

$$d_1^*, d_2^*, \dots, d_N^* = \arg \min \|T_{v_p w}\|_2. \quad (16)$$

This is a non-convex optimization problem that could have many local minima. Typically, one would attempt to solve the problem using a gradient descent technique [19]. In doing so, one would need to choose a starting point from which the optimization process may start. Given that for all positive d_1, d_2, \dots, d_N the closed-loop system is stable, any positive value may be considered acceptable. However, considering the structure of the system, it may be possible to find a set of damping ratios reasonably close to a minimum.

The transfer function $G_{vv}(s)$ in (3) is a high-order system of very lightly damped resonant modes. Depending on the geometry of the structure, these modes may be reasonably far away from one another. Given the highly localized nature of $Y(s)$, it may be a reasonable assumption to consider the effect of each individual bandpass section of the admittance on the specific mode of the base structure. Doing so, one may then search for a value of the damping ratio that would place the closed-loop poles of the system as deep into the left half of the complex plane as possible. A repeat of this procedure for every single mode that is to be controlled may result in a good starting point for the optimization problem (16).

8. Experimental results

In this section, we apply the above procedure to two flexible structures; the piezoelectric laminate beam described in [20], and the piezoelectric laminate plate described in [21]. The beam apparatus consists of a uniform aluminum bar with rectangular cross section and experimentally pinned boundary conditions at both ends. Likewise, the plate structure

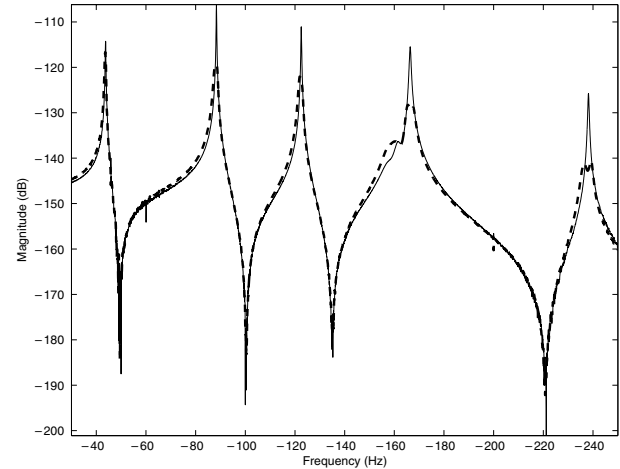


Figure 15. Experimental plate undamped (—) and damped (---) magnitude response of $G_{zw}(s)$.

also consists of an aluminum rectangular plate with pinned boundary conditions at all external edges.

The two experimental structures are shown in figures 7 and 8, respectively. For both structures, two piezoelectric patches (PIC151) are bonded to the surface in a collocated fashion using strong adhesive material, as shown in figures 9 and 10. On each structure, one piezoelectric patch is used as an actuator to generate a disturbance through the structure, and the other as a shunting transducer.

When observing the dynamics of a structure it is common practice to consider the transfer function between the displacement at a point on the structure $z(s)$ and the actuator voltage $w(s)$, $G_{zw}(s)$, as shown in figures 9 and 10, and also the dynamics between the shunting piezoelectric voltage and the actuator voltage, $G_{vv}(s)$.

Using a Polytec laser scanning vibrometer (PSV-300) and a Hewlett Packard spectrum analyzer (35670A), experimental frequency responses were obtained for $G_{zw}(s)$ and $G_{vv}(s)$. Using a subspace-based system identification technique [22], a model was fitted to the experimental data. The measured and identified magnitude responses are shown in figures 11 and 12. In the bandwidth of interest, the identified models were found to be good representations of the piezoelectric laminate systems.

The first four modes of the beam and the first six modes of the plate are to be controlled by a shunt impedance $Y(s)$ given in equation (9). Using the procedure explained in section 7, and the identified models, an optimal set of damping ratios for $Y(s)$ were determined for each structure. The admittances were digitally implemented, using the synthetic admittance circuit described in [12], and then applied to the shunt transducers. A comparison of the experimental undamped and damped experimental responses for $|G_{zw}(s)|$, are shown in figures 13 and 15. The experimental resonance magnitudes were successfully reduced, as summarized in table 1. Figure 14 shows the simulated closed-loop and open-loop poles. We can see from figure 14, that the closed-loop poles have been pushed further to the left on the real-imaginary plane.

It can be observed that the proposed impedances are very effective in reducing vibration of the base structures. However, their performance for the first mode is, in both cases, very

limited. This can be attributed to the locations at which the piezoelectric shunt transducers are placed on the beam and plate structure.

9. Conclusions

This paper suggests that the problem of piezoelectric shunt damping may be viewed as a feedback control problem in which the controller, itself, is inside an inner feedback loop. Based on this observation a new class of shunt systems was introduced. Using the feedback structure, the robustness properties of the shunted system were studied. Finally, the proposed method was experimentally verified on two structures.

Acknowledgments

This research was supported by the Australian Research Council and the Centre for Integrated Dynamics and Control (CIDAC).

References

- [1] Cudney H H 1989 Distributed structural control using multilayered piezoelectric actuators *PhD Thesis* SUNY Buffalo, New York
- [2] Lee C K 1987 Piezoelectric laminates for torsional and bending modal control: theory and experiment *PhD Thesis* Cornell University
- [3] Fuller C R, Elliot S J and Nelson P A 1996 *Active Control of Vibration* (New York: Academic)
- [4] Hagood N W and von Flotow A 1991 Damping of structural vibrations with piezoelectric materials and passive electrical networks *J. Sound Vib.* **146** 243–68
- [5] Hagood N W, Chung W H and von Flotow A 1990 Modeling of piezoelectric actuator dynamics for active structural control *J. Intell. Mater. Syst. Struct.* **1** 327–54
- [6] Wu S Y 1996 Piezoelectric shunts with parallel R – L circuit for smart structural damping and vibration control *Proc. SPIE Symp. on Smart Structures and Materials—Passive Damping and Isolation* pp 259–69
- [7] Wu S Y 1998 Method for multiple mode shunt damping of structural vibration using a single PZT transducer *Proc. SPIE Symp. on Smart Structures and Materials—Smart Structures and Intelligent Systems* pp 159–67
- [8] Wu S Y 1998 Piezoelectric shunts for simultaneous vibration reduction and damping of multiple vibration modes US Patent Specification 5, 783, 898
- [9] Behrens S and Moheimani S O R 2002 Current flowing multiple mode piezoelectric shunt damping *Proc. SPIE Symp. on Smart Structures and Materials—Damping and Isolation* (San Diego, CA, March 2002)
- [10] Hollkamp J J 1994 Multimodal passive vibration suppression with piezoelectric materials and resonant shunts *J. Intell. Mater. Syst. Struct.* **5** 49–57
- [11] Riodan R H S 1967 Simulated inductors using differential amplifiers *Electron. Lett.* **3** 50–1
- [12] Fleming A J, Behrens S and Moheimani S O R 2000 Synthetic impedance for implementation of piezoelectric shunt damping circuits *Electron. Lett.* **36** 1525–6
- [13] Tang J and Wang K W 2001 Active-passive hybrid piezoelectric networks for vibration control: comparisons and improvement *Smart Mater. Struct.* **10** 794–806
- [14] Dosch J J, Inman D J and Garcia E 1992 A self-sensing piezoelectric actuator for collocated control *J. Intell. Mater. Struct.* **3** 166–85
- [15] Alberts T E and Colvin J A 1991 Observations on the nature of transfer functions for control of piezoelectric laminates *J. Intell. Mater. Syst. Struct.* **8** 605–11
- [16] Halim D and Moheimani S O R 2001 Spatial resonant control of flexible structures—application to a piezoelectric laminate beam *IEEE Trans. Control Syst. Technol.* **9** 37–53
- [17] Khalil H K 1996 *Nonlinear Systems* 2nd edn (Englewood Cliffs, NJ: Prentice-Hall)
- [18] Hughes P C 1987 Space structure vibration modes: how many exist? Which ones are important? *IEEE Control Syst. Mag.* **7** 22–8
- [19] Luenberger D G 1969 *Optimization by Vector Space Methods* (New York: Wiley)
- [20] Behrens S and Moheimani S O R 2000 Optimal resistive elements for multiple shunt-damping of a piezoelectric laminate beam *Proc. IEEE Conf. on Decision and Control* (Sydney, Australia, Dec. 2000)
- [21] Halim D and Moheimani S O R 2003 Optimal placement of a piezoelectric actuator on a thin flexible plate using modal and spatial controllability measures *Mechatronics* 27–47
- [22] McKelvey T, Ackay H and Ljung L 1996 Subspace-based identification of infinite-dimensional multi-variable systems from frequency-response data *IEEE Trans. Autom. Control* **41** 960–79